

Hydrodynamic Analysis of Pipelines Transporting Capsule for Onshore Applications

Sufyan Abushaala
Faculty of Engineering
University of Misurata, Costal
Road, Misurata Libya

Abdulmonem Shaneb
Faculty of Engineering
University of Misurata, Costal
Road, Misurata Libya

Fatma Enbais
Faculty of Engineering
University of Misurata, Costal
Road, Misurata Libya

Adel Abulifa
Faculty of Civil Aviation ,
Misurata Libya

s.abushaala@eng.misuratau.edu.ly

Abstract— Rapid depletion of energy resources has immensely affected the cargo transportation industry. Efforts have been made to develop newer economic and environmental friendly modes for this purpose. Bulk solids can be transported for long distances effectively in pipelines. Raw materials can be stored in spherical containers (commonly known as capsules) transported through the pipeline. For economical and efficient design of any transportation mode, both the local flow characteristics and the global performance parameters need to be investigated. Published literature is severely limited in establishing the effects of local flow features on system characteristics of Hydraulic Capsule Pipelines (HCPs).

The present study focuses on using a well-validated Computational Fluid Dynamics (CFD) based solver to simulate the unsteady turbulent flow of a spherical capsule as a simplified case in HCPs for onshore applications. A novel numerical model has been employed in the present study with the aid of the dynamic mesh technique for calculating the pressure and the velocity variations within such pipelines. The numerical model comprises a straight test section. The numerical model for capsule flow yields realistic results for the global flow parameters as compared to the experimental data from the test rig developed in the present study. The influence of the carrying fluid (water) on the capsule has been verified by estimating the shear forces and the friction coefficient. In addition, novel models have been developed for predicting the wet friction coefficient considering the start-up effect in such systems.

Index Terms: Computational Fluid Dynamics (CFD), Hydraulic Capsule Pipelines (HCP), Dynamic Mesh technique, Hydrodynamics of Capsule Flow, Six-Degrees-of-Freedom (6DOF), User-Defined Function (UDF), Transient Effect.

I. INTRODUCTION

Pipelines transporting capsules are becoming popular amongst cargo and transportation industries throughout the world.

The capsules are hollow containers filled with different materials such as minerals, ores etc. In some cases, the material that needs to be transported can be shaped as capsules themselves. The shape of the capsules can be spherical, cylindrical or rectangular with different design considerations depending on the required application. Primarily, there are two different applications of hydraulic capsule pipelines i.e. onshore and offshore. Onshore applications comprise mostly horizontal pipes, while offshore applications comprise primarily of vertical pipes. Pipefittings, such as pipe bends etc., are an integral part of any piping system. For an effective design of any system, interdependence of a large number of geometrical and flow variables could to be investigated. This information is not explicitly available in the literature, especially for pipelines transporting spherical capsules. Hence, this study provides an introductory discussion regarding water flow and capsule flow in pipelines.

The concept of the flow of capsules in pipelines has been proposed in the early 1960s as a practical means for the large-scale transport of solids in a pipeline. Capsule pipelines transport materials or cargos in capsules propelled by fluid. Either the cargos may be contained in capsule, or the cargos may be shaped as capsules. In either ways, the transportation process can be carried out for two different applications. In the first application, the process takes place under the surface of the earth (onshore), in which the pipelines are primarily horizontal.

The hydraulic capsule pipelines (HCPs) is a new technology compared to the pneumatic capsule pipelines (PCPs). The British Authority was the first to consider (PCPs) for military use during the Second World War. Military authority proposed to use HCPs to transport supplies and even troops in Burma. Hydraulic capsule pipeline is an emerging technology by which the freight is transported in hollow containers suspended by a fluid, usually water, propagated through a pipeline. This technology is very famous in coal transportation, and such pipelines are known as Coal-Log Pipelines (CLPs) [1]. Generally, the shape of the capsule is normally cylindrical or spherical. The economic surveys have revealed that the capsule transportation is more economical than conventional methods of transporting goods such as trucks, rails etc. Such pipelines also provide additional high levels of efficiency and reliability compared to those old methods for transportation [2].

Received 11 Nov, 2018; revised 26 Nov, 2018; accepted 28 Nov, 2018.

Available online November 29, 2018.

The characteristics of the capsule flow and the capsule flow motion are important concerns. Although various researchers have studied the hydrodynamics of HCPs extensively; however, many basic and crucial questions remain. One is how to predict the pressure variations along a capsule that is either stationary or moving in a pipeline as this information is vital to the design of pipe systems. Many researchers have investigated the pressure drop or head loss along a capsule pipeline and have reported their findings in the literature assuming that design parameters are constant. Those assumptions are hence valid only for limited conditions i.e. concentric flow, laminar and turbulent flow or very long capsules. However, the wet contact friction coefficient is not constant and it varies widely with many parameters in an unpredictably manner. The wet contact friction coefficient cannot be accurately predicted unless there are a set of equations that have greater generality for a wide range of operation conditions and a wide range of designing parameters.

Capsule flow in pipelines is a transient phenomenon and the capsules trajectory varies under influence of the local flow structure. A numerical study on the transient behavior of the capsules in the pipelines has been carried out. The study accommodates the unsteady effect in the straight pipes. The study has provided precious information regarding the generation of complex flow structures in the pipelines transporting spherical capsules in both space and time domains. Furthermore, transient analysis of pipelines transporting spherical capsules conducted in this study has provided information regarding the trajectory and the orientation of the capsules along with the translational velocity and acceleration. Transient modelling enables development of prediction models that incorporate transient effects such as start-up requirements.

The transition in the capsule motion from resting on the pipe bottom floor to levitating in the flow stream is considered as the most important factor. The changes in the flow structure during this stage is very complex, so that study has been primarily conducted to understand the hydrodynamic analysis of pipelines transporting capsule for onshore applications. This includes the behavior of the capsule during the starting-up process to the steady flying stage. However, studies on the dynamic capsules flow under unsteady isothermal conditions are severely limited and hence are the motivation of this work.

II. COMPUTATIONAL MODELLING

Applications of computational fluid dynamics (CFD) to the industry continue to grow as this advanced technology takes advantage of the increasing speed of computers. In the last two decades, different areas of flow simulation including grid generation techniques, solution algorithms, turbulence models, and computer hardware capabilities have witnessed tremendous development offering a cost-effective solution to many engineering problems. In this study, ANSYS FLUENT® has been

used to model the flow of a sphere in a hydraulic pipe, when the flow is turbulent.

The pre-processing in CFD is broken into two main steps, i.e. creation of the geometry and the meshing of the flow domain. This section provides more details of these two steps.

A. Geometry Creation

A pipe of 0.1m diameter fully filled with water of a length of 2m is considered. The first half of the pipe is considered as the area of interest (the test section), and the second half is representing the outlet pipe. The test section been used for the flow diagnostics of capsule transport is 1m long and it has the same properties as that studied by T. Asim [3]. The pipe in Figure. 1 is considered to be hydro-dynamically smooth. The capsule has been presented as a sphere of different sizes positioned near the pipe entrance. This numerical test setup has been used throughout the entire this study for the analysis purposes. The geometries of both pipe and capsule have been created using the Design Modeler facility in ANSYS 17.1.

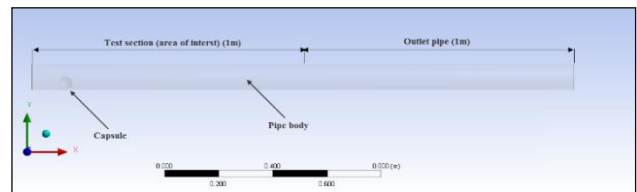


Figure. 1. The Pipe Geometry

B. Meshing the Flow Domain

The area of interest (the test section) of the pipe has been meshed with tetrahedral elements. As it can be clearly seen from Figure. 2, inflation has been adopted for the geometry mesh with a first layer thickness of 0.003938m of three layers around the capsule for better flow analysis. FLUENT has been used for the grid generation with face sizing of 1mm around the capsule, and the resulted grid consists of around two million elements.

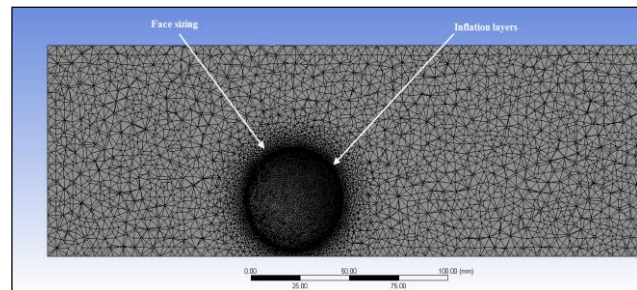


Figure. 2. Meshing of the Flow Domain

For unstructured grids, the computation time associated with re-meshing may therefore become excessive. In addition, the re-meshing suffers from an accuracy loss in the physical conservation laws, where the local computational accuracy will possibly be reduced due to drastic grid size variation. However, for relatively high Reynolds numbers as in this study, the computation will

become expensive because of the fineness of the grid that is required to resolve the flow behavior in the boundary layer region. This has been considered in the simulation by separating the layers around the capsule. These layers will not be deformed or re-meshed.

The motion of the boundaries can be rigid such as the capsule moving in a pipeline filled with water, or deforming such as the interior around the capsule as shown in Figure. 3. In either case, the nodes that define the cells in the domain must be updated as a function of time, and hence the dynamic mesh technique solutions are inherently unsteady. Whenever the capsule and its surrounding layer mesh are displaced, the mesh outside the boundary layer is smoothed and re-meshed.

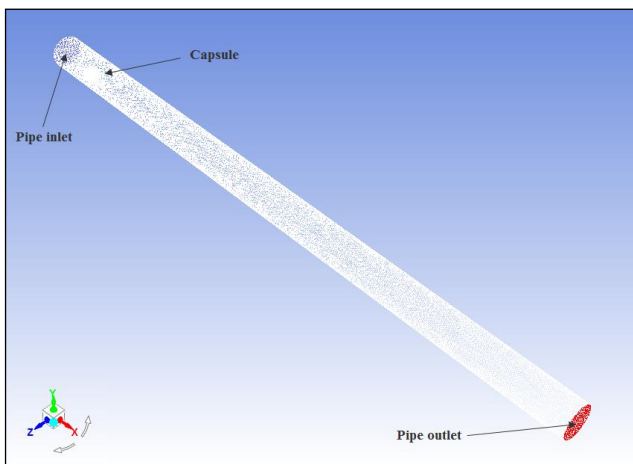


Figure. 3. Mesh Associated with a Moving Spherical Capsule

III. DYNAMIC MESH TECHNIQUE

The dynamic mesh is an embedding technology that has been used for simulations that require simplifying the grid generation for complex geometries [4]. The mesh deforms at each time step with respect to the specified motion rather than that the whole mesh system is regenerated. This approach allows preserving the grid topology, i.e., the grid connectivity is maintained during the deformation. The dynamic mesh technique, particularly for capsule flow simulation, has been proposed in the present study using an unstructured mesh that locally coupled with six-degrees-of-freedom (6DOF) solver. The built-in (6DOF) solver is available for applications with unconstrained motion, such as the capsule motion in this study.

The dynamic mesh technique can be applied to single or multiphase flows and can be used for steady-state applications when it is beneficial to move the mesh in the steady-state solver. To simulate a flapping-wing system, the relatively large displacement, such as rotation, translation events during the flight would significantly challenge the existing mesh deformation techniques. The motion can be either a prescribed motion or an un-prescribed motion where the subsequent motion is determined based on the solution at the current time. ANSYS FLUENT® handles updating the volume mesh automatically at each time step based on the new positions of the boundaries. To use the dynamic mesh, a

starting volume mesh and the description of the motion of any moving zones need to be provided. ANSYS FLUENT allows describing the motion using both boundary profiles and user-defined functions (UDFs).

A. User Defined Function and Contact Detection

ANSYS FLUENT also allows defining some custom properties of a wide range of moving objects in different applications. Different commands can be used to specify those properties for the six-degrees of freedom (6DOF) solver in FLUENT including mass, moment, products of inertia and external forces and moment properties if applicable. The properties of an object can consist of multiple zones and it can change with time if desired, depending on the analysis undertaking and on the targeted application. The properties can be provided, interpreted or compiled to the solver via a User Defined Function (UDF) which can be achieved using C programming [5].

The wall of the capsule undergoes a rigid body motion and displaces according to the calculation performed by 6DOF solver. The contact between the capsule wall and the pipe wall is controlled by the aid of the contact detection feature provided by ANSYS Fluent in order to avoid the direct contact and breaching the continuity in the mesh domain.

Time step size has been judged depending on the estimation rule introduced in FULENT ANSYS guide [6]. Different time step sizes have been estimated and verified to be sufficiently enough for time independent solutions. The estimation has been made depending on the smallest grid size and the operating velocity (the smallest grid cell divided by the average flow velocity). According to the estimation made, the time step was about 1×10^{-3} for average flow velocity of 1m/sec. This value may decrease as the average operating velocity increases. The calculations start from an initial flow field obtained from a well-converged steady state computation where the capsule is positioned near the test section entrance 1.5mm away from the bottom wall. Regarding the convergence criteria, the residual for the continuity equation is set to be less than 10^{-5} . During each time step, variations should be resolved by having at least 20 time steps. The correctness of the time-step is verified if the continuity residual drops about two orders of magnitude from the beginning of the time-step within 20 iterations.

B. Material Properties and Boundary Conditions

In the present study, the investigations have been carried out in a hydraulic pipeline transporting capsules where the capsules may have different densities. The fluid medium within the pipe has been defined as liquid-water with a density of 998.2 kg/m^3 and dynamic viscosity of 0.001003 kg/m.s . The capsule used in the current study may have different densities. The capsule is called equi-density capsule if the capsule density is similar to that for water, and it is called high-density capsule if the capsule density is greater than the water density. The operating conditions being given to the solver are the operating pressure of 101325 Pa (i.e. atmospheric pressure), and a gravitational acceleration of 9.81 m/sec^2 is activated

working downwards. The boundary types that have been specified in the present study are illustrated in Table.

The capsule and the pipe wall have been presented as walls with no slip conditions. The capsule interacts with the carrier fluid when the flow takes place. The wall of the capsule undergoes a rigid body motion and displaces according to the calculations performed by 6DOF solver. The pipeline inlet has been treated as a velocity inlet. The pipe outlet has been treated as a pressure outlet and it has been kept at atmospheric pressure. The pipe has been considered as a hydro-dynamically smooth pipe having a wall roughness constant of zero. A zero-gauge pressure has been set for the pressure outlet boundary condition, and the intensity of turbulence is 5% at inflow boundaries for 0.1m hydraulic diameter of the pipe.

Table 1. Named Selections for the Boundary Conditions

Boundary Name	Boundary Type
Inlet to the Pipe	Velocity Inlet
Outlet of the Pipe	Pressure Outlet
Wall of the Pipe	Stationary Wall
Capsules	Translating Walls in the direction of the flow

IV. SOLVER IMPLEMENTATION

The software used in the present study is called Fluent, which is an integral part of CFD package ANSYS 17.1. The default standard algorithm Semi-Implicit Method for Pressure-Linked Equations (SIMPLE) has been used in the simulation process. This algorithm may reduce the computation and a quick convergence can be obtained. The details of the solver settings used in the present study have been presented in the following sections.

A. Governing Equations

Newton's second law states that the rate of change of momentum of a fluid particle equals the sum of the forces on the particle. There are two types of forces on fluid particles. These are surface forces and the body forces. Surface forces include pressure, viscous and gravity forces while body forces include centrifugal, Coriolis and electromagnetic forces. It is a common practice to highlight the contributions due to the surface forces as separate terms in the momentum equations and to include the effects of body forces as source terms. The carrying fluid (water) in the pipe has been treated as an incompressible fluid. The flow can then be computed from the continuity and the momentum equations.

B. Model Selection

The velocity of the flow within hydraulic pipelines is such that the compressibility effects can be neglected. Therefore, a pressure-based solver has been selected for solving the capsule flow. There are many models available in the commercial CFD packages to model the

turbulence, each one of those models has its own advantages and disadvantages. As far as the transport of capsules in a pipeline is concerned, due to the formation of a wake region downstream of the capsule, and the flow separation, k-ε model has been chosen for predicting the turbulence in such pipelines [8]. The primary reason behind choosing k-ε model is its supremacy in accurately simulating the wake regions.

The k-ε model belongs to the class of two equation models and it solves one transport equation for turbulent kinetic energy k and another for dissipation rate ε [9]. k-ε model is relatively simple to implement and leads to stable calculations that converge easily in many applications; however, it is valid only for fully turbulent flows. Realizable k-ε model shares the same turbulent kinetic energy equation as the normal k-ε model with an improved equation for ε. It has an improved performance for flows involving boundary layers under strong adverse pressure drops or separation, rotation, recirculation and strong streamline curvature [6].

The k-ε family is not valid in the near-wall region, whereas Spalart-Allmaras, for example, and k-ω models are valid all the way to the wall providing a sufficiently fine mesh. In this study, the Enhanced Wall Treatment option has been used to overcome this issue. Enhanced Wall Treatment option is suitable for low Reynolds flows with complex near-wall phenomena where turbulent models are modified for the inner layer (both the buffer layer and the viscous sub-layer) [10]. However, it generally requires a fine near-wall mesh capable of resolving the viscous sublayer, which has been handled by adding inflation layers, and face sizing around the capsule.

C. Near Wall Treatment

Turbulent flows are significantly affected by the presence of walls; i.e. capsule wall in this study. Viscous damping reduces the tangential velocity fluctuations very close to the wall, while kinematic blocking reduces the normal fluctuations. However, the turbulence is gradually amplified due to the large gradient in the mean velocity [7]. The near-wall treatment affects the fidelity of numerical solutions, and therefore an accurate representation of the flow in the near-wall region determines successful predictions of wall-bounded turbulent flows.

The k-ε model is thought to be primarily valid for turbulent core flow as it is in this study, thus considerations need to be given in order to make this model suitable for wall-bounded flow. FLUENT provides the near-wall approach with the enhanced wall treatment option. It has been ensured that the y^+ value is under 5 in the viscous sub-layer, between 5 and 12 in the buffer layer and more than 12 in the log-law layer. This will ensure resolving the boundary layer around the capsule with a reasonable accuracy for this particular case. The y^+ value has been calculated from [7].

$$y^+ = \frac{\rho_w u_* y}{\mu_w} \quad (1)$$

where u_* is the friction velocity at the nearest wall and y is the nearest wall distance. The friction velocity has been computed from [7].

$$u_* = \sqrt{\frac{\tau_{wall}}{\rho_w}} \quad (2)$$

Where τ_{wall} is the wall shear stress. Equations (1) and (2) have been used to compute wall shear stress from the numerical prediction models. By keeping y^+ values under a suitable number, y values can be then estimated and specified as the first layer thickness. Many numerical experiments have been conducted to justify the proper number of mesh cells needed for solving the inner region (this includes the buffer layer and the viscous sublayer). Few iterations have been carried out for the model to judge the accuracy depending on the resultant shear stress on the capsule wall until it falls within at least 8% error. The results led to a first sublayer of 0.001389m granting two cells in the viscous sublayer, one in the buffer layer and two cells in the outer region (the log-law layer).

D. Mesh Independency

Two different meshes with one million and two million mesh elements were selected for primary mesh independence testing. The results obtained, shown in Table 2 depicts that the difference in the pressure drop is less than 5% between the two meshes under consideration. It can therefore be concluded that the mesh with one million elements is capable of accurately predicting the flow features and it is reliable to conduct any further analysis.

Table 1. Mesh Independency Results

Number of mesh elements (Millions)	Pressure at the inlet (Pa)	Pressure at the outlet (Pa)	Pressure drop (Pa/m)	Difference (%)
1M	379.99	116.06	263.92	3.71
2M	406.81	133.07	273.74	

V. EXPERIMENTAL WORK

A flow loop has been designed and built with the means of a 3m long transparent test section of 2" (50mm) inner diameter as it can be seen in Figure. 4. The experiment setup has been established to acquire data for validating the numerical model developed in this study and for future work. The pipes and the pipes fittings used in building the flow loop are made of clear impact resistant polyvinyl chloride (PVC) with maximum operating pressure of 16bar. The centrifugal pump has a maximum operating pressure of 16bar at a maximum pumping fluid temperature of 120°C and at a maximum ambient temperature of 40°C. The rated power of pump's motor is 37kW at 2900rpm, where the efficiency of the motor ranges from 92% to 93.7%, whereas the minimum efficiency index (MEI) of the pump is ≥ 0.4 . Pump's flow rate has been varied to get appropriate V_{av} values. This is achieved through the use of an 11kW Siemens Optima Pump Test Rig which has a flexible and sophisticated control system. This system is integrating a programmable logic controller and human interface to

enable specific timing and control setting functions to operate the pump's rotational speed automatically. The centrifugal pump is connected to the capsule injection system via a digital turbine flow meter.

Two long-range optical (OPB720A-06Z) sensors have been installed on the measuring section where the flow is fully developed with a spacing of 0.5m between them. The signals are transmitted to the computer through a printed circuit board via an externally powered USB data acquisition system (NI-USB-6353, X Series DAQ). The printed circuit board is interfaced to the computer using a system-design platform supported by LabVIEW visual programming language. The output data have been evaluated and then used to compute the capsule velocity and the pressure drop.

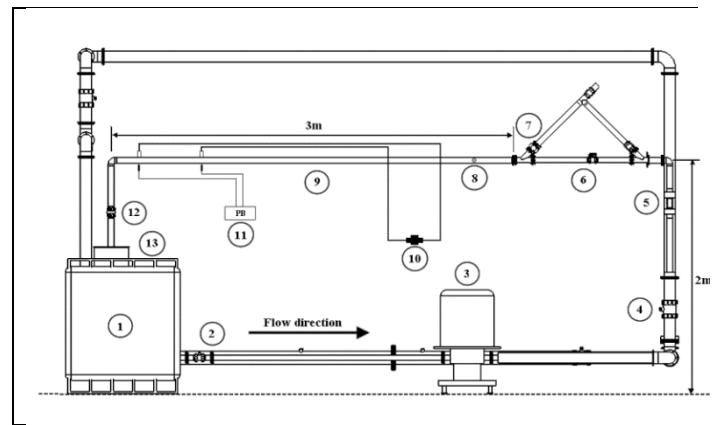


Figure. 4 Schematic Diagram of the Experimental Set-up; (1)-Main Water Tank, (2)-Main tank Outlet Valve, (3)-Centrifugal Pump, (4)-Loop Main Valve, (5)-Flow Meter, (6)-Capsule Injection Mechanism, (7)-Gate Valve, (8)-Capsule, (9)-Test Section, (10)-Pressure Transducer, (11)-Optical Sensors, (12)-Loop Outlet Valve, (13)-Capsule Ejection Mechanism

Once the capsule is fed into the capsule injection system, while the secondary loop is shut, the pneumatic knife gate valve is opened leading the capsule into the primary loop. The capsule is then collected on the top of the water tank from the capsule ejection mechanism, while the water is drained into the tank.

The capsule bodies are made of three different capsule to pipe diameters ($k = 0.5, 0.6$ and 0.7) in order to study the effect of diameter ratio. Capsules of density greater than that for the carrying fluid are fabricated from raw materials; PVDF and Aluminum, whereas capsule with density equal to that of carrying fluid are 3D printed and filled with honey in order to obtain the correct density. Accordingly, nine spherical capsules have been made of different materials with various sizes.

A. Computing the Average Flow Velocity

The average flow velocity V_{av} has been computed according to Equation (3) [11].

$$V_{av} = \frac{\text{Flow rate}}{\text{Pipe cross sectional area}} = 0.008162 \times Q \left(\frac{m}{sec} \right) \quad (3)$$

Where Q is the flow rate in $\frac{l}{min}$.

During the experiments, the water flow rate was adjusted whilst the capsule was held in the injection system prior to the test section. In most cases, the flow rates remain constant whether or not the capsule is moving or stationary. Larger and heavier capsules present more resistance to the flow, so they affecting the flow rate but not for long. The flow becomes fully developed at 2.5m away from the injection section.

B. Computing the Capsule Local Velocity

The steady state capsule velocity is reached when it passes between the two measuring stations within the measuring section. This refers actually to the local capsule velocity at the measuring section between the two stations of a known distance. The capsule velocity can be calculated from [11].

$$V_c = \frac{\text{Distance between the two stations}}{\text{Capsule passage time}} = \frac{0.5}{t} \quad \left(\frac{m}{sec}\right) \quad (4)$$

Where 0.5 refers to the distance between the two stations in meters. The capsule passage time used in the Equation (4) is obtained from the output spreadsheet from the data acquisition system. The time t refers to the time between two detection instances in the detection history record. Figure. 5 shows an example for a heavy density spherical capsule of a value of k equal to 0.6 at an average operating velocity of 2m/sec.

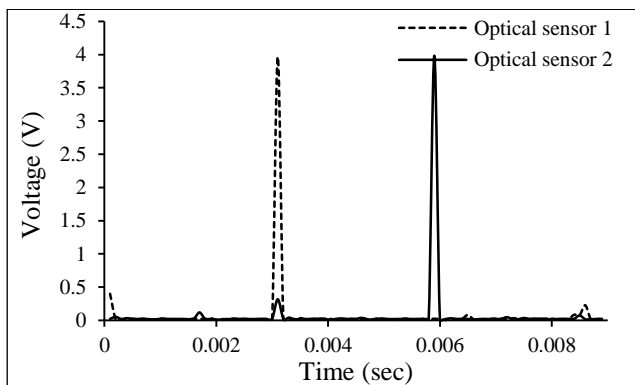


Figure. 5 Detection History for a Spherical Heavy Density Capsule of k Equal to 0.6 at 2m/sec

It can be clearly seen that the optical sensors detected the capsule (first spike at 52.46sec), and then the second sensor detected the capsule (second spike at 52.18sec). Thus, the travelling time between the two stations can be presented as the travelling time between two stations, i.e. $52.46 - 52.18 = 0.28$ seconds. From Equation (4) the capsule local velocity can be calculated as $V_c = \frac{0.5}{0.28} = 1.78 \left(\frac{m}{sec}\right)$.

C. Computing the Pressure Drop

All pressure drops have been recorded for two cases; pressure drop due to fluid (single phase), and the pressure drop due to the capsule. The individual pressure drop per unit length can be expressed as $\Delta P/L$.

$(\Delta P/L)_c$ and $(\Delta P/L)_w$ refer to the pressure drop per unit length due to the capsule (solid phase) and due to the carrying fluid only (single phase) respectively.

The sum of those two drops is the total pressure drop or the pressure drop of the mixture per unit length. Where L is the distance between the pressure taps. The measuring system has been also used to estimate the pressure drop per unit length due to the fluid only (single phase) in order to check the reliability of the system. Figure. 6 depicts the pressure drop per unit length measured and plotted against the pressure drop per unit length from the theory $\Delta P = f \frac{\rho V^2}{2D}$ for the single phase. The friction coefficient f is estimated from $f = \frac{0.316}{Re_w^{1/4}}$. The system showed a good agreement with the theoretical values for the pressure drop at the particular case with a percentage error less than 5%.

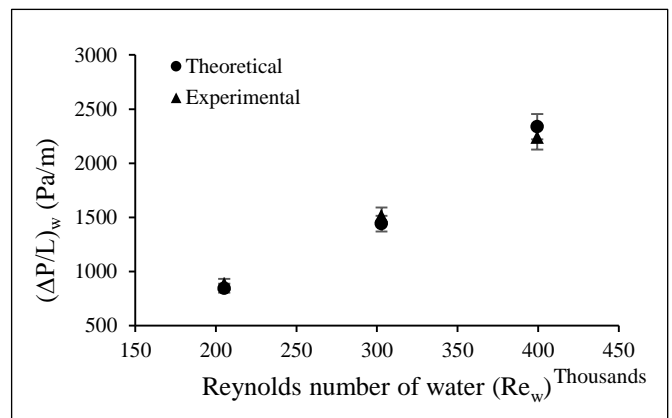


Figure. 6 Pressure Drop per Unit Length Across the Test Section for the Single Phase

Here is an example for calculating the pressure drop per unit length for the mixture. The pressure drop per unit length for the mixture has been calculated by the means of the total area under the curve $(\Delta P/L)_m = \int_0^{0.8} \left(\frac{\Delta P}{L}\right)_m (t) dt$. Fig.7 illustrates the pressure drop history per unit length of the mixture due to a heavy density spherical capsule of k equal to 0.6 at an average flow velocity of 2m/sec. By applying the area under curve equation, the pressure drop per unit length will be 986.43Pa/m.

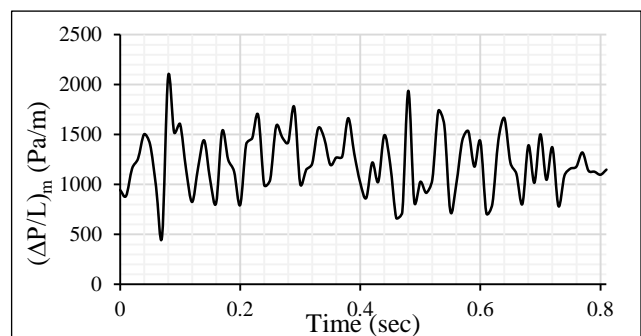


Figure.7 Pressure Drop History of the Mixture per Unit Length due to a Heavy Density Spherical Capsule of k Equal to 0.6 at V_av Equal to 2m/sec

VI. RESULTS AND DISCUSSION

The results from the onshore numerical models have been presented in here starting with the model verification to the flow field characterization in HCPs. A detailed qualitative and quantitative unsteady analysis has been carried out for better understanding of the flow complexity. The effect of geometric parameters and flow conditions have also been investigated. Finally, a novel model has been developed for predicting the friction coefficients.

A. Model Verification

One of the most important steps while conducting numerical studies is the benchmarking of the results. This means that some of the results obtained from the numerical simulations are compared against experimental findings to confidently authorize that the numerical model represents the physical model of the real world. Hence, all the geometric, flow and solver-related parameters/variables become important in benchmarking studies. For the current study, the numerical model has been validated against the experimental findings for both the pressure drop and the capsule velocity in a pipeline carried out by the author. The numerical model has been set for the conditions listed in Table 2

Table 2. Validation Tests

Name/property	Value/Range/Comment	Units
Specific gravity	1	N/A
k	0.5	N/A
V_{av}	2, 3 and 4	m/sec
N	1	N/A

Further to the previously mentioned discussion regarding the model verification, the cases in Table 2 have been numerically solved. Figure. 8 depicts the variations in the pressure drop within the pipeline, from both CFD and experiments, at various flow velocities, for the flow of equi-density spherical capsules in a horizontal pipeline. It can be seen that the CFD results are in close agreement with the experimental results, with an average variation of less than 10%.

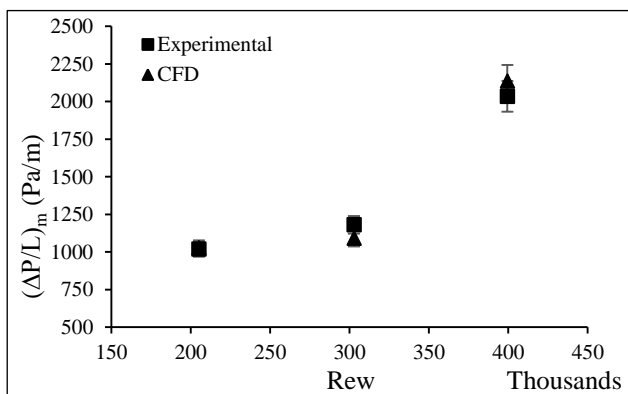


Figure. 8 Validation of the CFD Results Against the Experimental Results for the Pressure Drop due to an Equidensity Spherical Capsule of k Equal to 0.5 at Various Flow Velocities

Moreover, Figure. shows the variations in the capsule velocity within the pipeline, from both CFD and experiments, at various flow velocities, for the flow of equi-density spherical capsules in a horizontal pipeline. It can be seen that the CFD results are in close agreement with the experimental results, with an average variation of less than 5%.

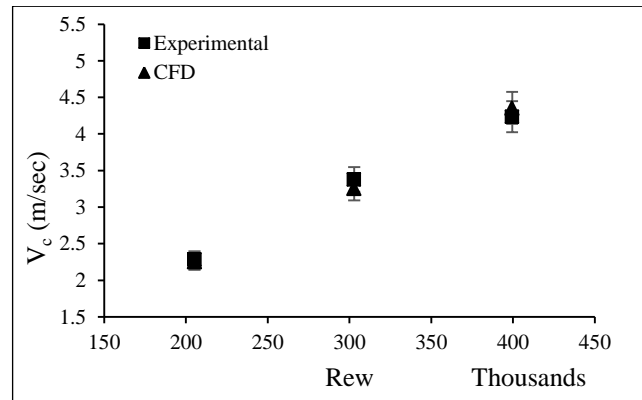


Figure. 9. Validation of the CFD results against the experimental results for the Velocity of an Equidensity Spherical Capsule of k Equal to 0.5 at Various Flow Velocities

It can be concluded that the proposed numerical model is capable of represent the physical model of a pipeline transporting capsules. The same model has been used for simulating the various cases concerning the flow of capsules in horizontal pipelines including bends.

B. Flow Field Characterisation

Figure. 10 depicts variations in pressure for the flow of an equi-density single spherical capsule of k equal to 0.5 in a horizontal pipe at $V_{av} = 1\text{m/sec}$. It can be seen that the position of a capsule changes the pressure distribution. The pressure gradients near the capsule are severe at the beginning of the capsule motion. At this stage, the pressure of water increases from 200Pa to 850Pa as it approaches the capsule. This happens due to the additional resistance offered by the stationary capsule to the flow. As the capsule starts moving, the flow passes through the annulus between the pipe wall and the capsule offering less resistance to the flow. Near the steady flying, the pressure gradient stabilizes and the capsule reach the equilibrium stage.

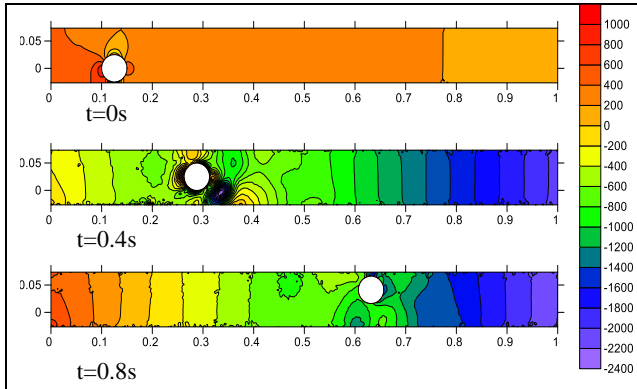


Figure. 10 Variations in Pressure for the Flow of an Equidensity Single Spherical Capsule of k Equal to 0.5 at V_{av} Equal to 1m/sec

Figure. 11 shows the spatial distribution of the pressure drop for an equi-density spherical capsule of k equal to 0.5 in a horizontal pipe at $V_{av} = 1\text{m/sec}$. The variations of pressure drop have been measured between the pipe inlet and outlet, and then have been plotted in a dimensionless form. The pressure drop changes depending on the capsule location. The pressure drop is very high initially at the beginning of the capsule motion. The capsule elevation oscillates before the capsule approaches its equilibrium configuration. It can be seen that during the motion of the capsule, the pressure drop values oscillate before attaining a constant value.

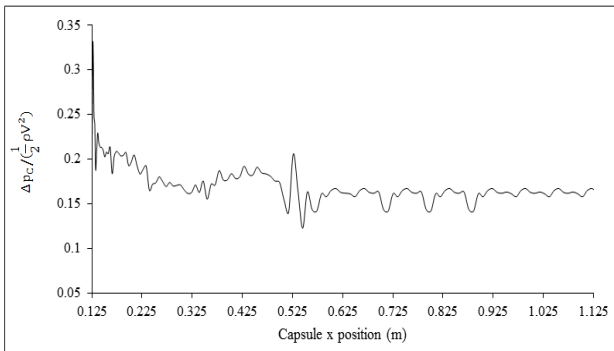


Figure. 11 The Spatial Distribution of the Pressure Drop for an Equidensity Capsule of k 0.5 in a Horizontal Pipe at $V_{av} = 1\text{m/sec}$

Figure. 12 shows the distribution of pressure on the capsule surface in a non-dimensional form Equation (5). The ordinate of the graph is the dimensionless pressure coefficient at 360 locations on the capsule surface starting from the top of the capsule with respect to flow time. From the detailed pressure distribution, it can be seen that the pressure distribution on the capsule is non-uniform. The maximum pressure occurs at 180° (behind the capsule), and the minimum at 270° (underneath the capsule) in the initial stage of motion. However, the distribution becomes uniform as the capsule nears the equilibrium stage. The pressure coefficient can be represented as [3].

$$C_p = \frac{P - P_\infty}{\frac{1}{2} \rho_\infty V_\infty^2} \tag{5}$$

Where P represents the pressure at a point, P_∞ refers to the free stream pressure, ρ_∞ is the density of the fluid at the free stream location and V_∞ is the velocity of the fluid at the free stream location. The pressure coefficient C_p can be defined as the pressure at a given location in the flow field, with respect to an undisturbed point, in a dimensionless form. The pressure coefficient is usually used to represent the pressure distributions around a bluff body for instance. The flow parameters near the capsules are dependent on the shape and size of the capsules; hence, C_p has been used to analyze the flow near the capsules.

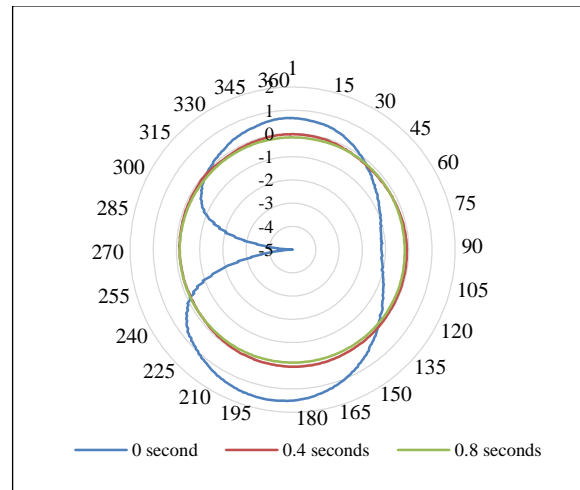


Figure. 12 The Pressure Distribution on the Surface of an Equi-Density Spherical Capsule of k Equal to 0.5 at V_{av} Equal to 1m/sec

Figure. 13 depicts the variations in the velocity magnitude in a horizontal pipe transporting a single equi-density spherical capsule of k equal to 0.5 at an average flow velocity of 1m/sec. It can be seen that the velocity of the capsule changes as the capsule starts to move. At the initial capsule position, the carrier fluid flow velocity increases in the cross-sectional area of the flow through annulus between the capsule and the pipe wall. The flow velocity then drops in the center of the pipe as the flow exits the annulus. This extreme gradient in velocity presented in the annulus regions gives rise to shear forces acting on the capsule. Both shear and pressure forces keep acting until the capsule reaches equilibrium. At this stage, the velocity gradient becomes less.

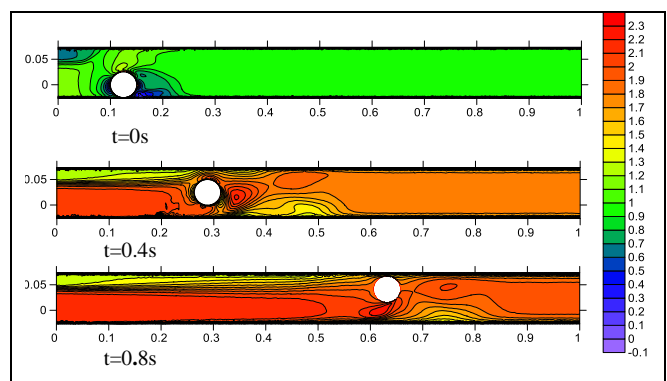


Figure. 13 Variations in the Velocity Magnitude for a Single Equidensity Spherical Capsule of k Equal to 0.5 at $V_{av} = 1\text{m/sec}$

Figure. 14 depicts the capsule velocity history of an equi-density capsule having capsule to pipe diameter ratio of 0.5 at an average inlet velocity of 1m/sec in a horizontal hydraulic capsule pipeline.

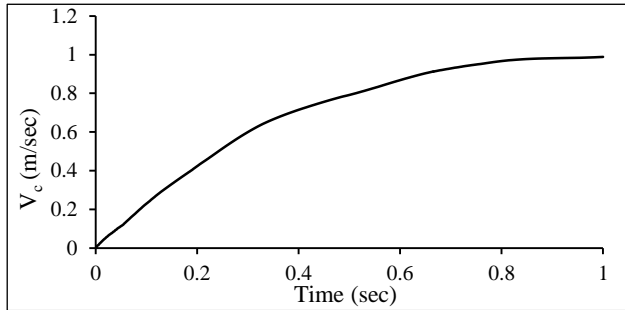


Figure. 14 The Velocity History of a Single Equidensity Spherical Capsule of k Equal to 0.5 at V_{av} Equal to 1m/sec

At this water average inlet velocity, the capsule attains a constant velocity in short time after starting from standstill position. The results show that the capsule velocity is higher than the water velocity when the capsule reaches the near steady state. The unsteady flying time is approximately 0.6sec as the capsule velocity starts stabilizing just after this time even if it is allowed to run more.

Forces acting on the capsule are the pressure and shear forces. The numerical model is capable of estimating those forces.

Figure. shows total acceleration history for an equi-density spherical capsule of k equal to 0.5 at an average flow velocity of 1m/sec in a horizontal pipe. The graph depicts the total acceleration due to pressure and shear forces. The total acceleration is mostly in x-direction only as the most capsule motion is considered in x-direction. The capsule tends to have a considerably high acceleration in the beginning of the capsule motion and it attains a constant velocity in a short time.

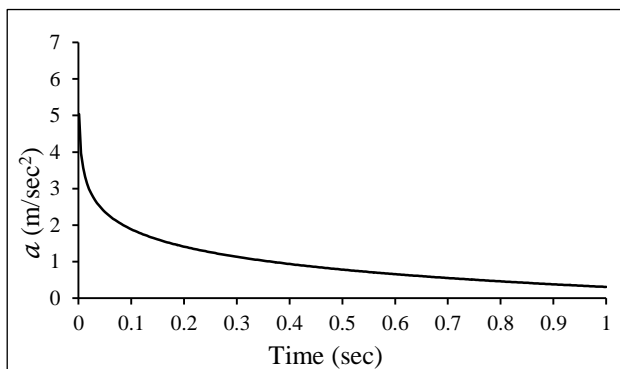


Figure. 15 The Total Acceleration History Due to Pressure and Shear Forces for an Equidensity Spherical Capsule of k Equal to 0.5 at an Average Flow Velocity of 1m/sec

The motion of a capsule in a horizontal pipeline can be determined by three non-dimensional parameters;

Reynolds number Re , capsule to pipe diameter ratio k and capsule material specific gravity s . An efficient way to study the effect of those parameters is to examine the effect of each parameter while holding the other two constant. However, mostly none of the results obtained in the literature have been presented followed such a framework. In the context of experimental research and practical operations, it is more natural to vary the fluid velocity and observe the behavior of the capsule while other properties, such as the capsule density and its size, are fixed.

Based on the results obtained, a novel semi-empirical prediction model for the friction coefficient has been developed. All the capsule sizes and densities included in the investigation have been involved in the formulation of prediction models.

C. Friction Coefficient Prediction Model

The friction coefficient for water flow and capsule flow [12] separately can be calculated by the following expressions.

$$f_w = 0.0055 + \frac{0.55}{R_w^3} \quad (6)$$

And

$$f_c = 2D \frac{\left(\frac{\Delta P_m}{L_p} - \frac{\Delta P_w}{L_p}\right)}{\rho_w L_p V_{av}^2} \quad (7)$$

Using multiple variable regression analysis, semi-empirical expression for the prediction of friction coefficient due to the presence of a single spherical capsule has been developed. This prediction model is shown in Equation (8) and it is applicable for horizontal hydraulic pipes carrying a single spherical capsule. The model is based on the maximum pressure drop obtained from the numerical simulations. This will help to overcome the starting up requirements for operating the pipelines transporting spherical capsules. This will allow including the steady flying stage of the capsule flow pumping requirements.

$$f_c = 32.28 \times 10^6 \left[\frac{k^{4.511} * (s+1)^{1.998}}{Re_c^{1.881}} \right] \quad (8)$$

Figure. shows the difference between the friction coefficients, due to a single spherical capsule in horizontal pipelines, calculated using the expressions presented in Equation (8) and that obtained from the CFD results in this study to approve the helpfulness of these semi-empirical expressions. From the same figure, it can be clearly seen that more than 80% of the data lies within $\pm 20\%$ error bound of the semi-empirical expression for spherical capsules.

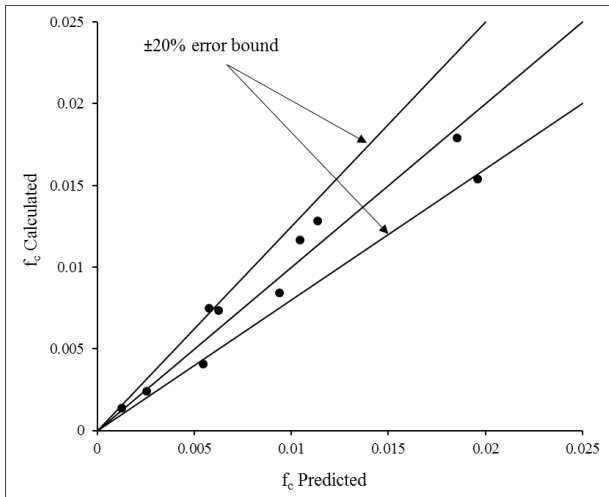


Figure. 16 Results from Multiple Regression Analysis for the Friction Coefficient of a Single Spherical Capsule

VII. CONCLUSIONS

This study provided a numerical model for the unsteady analysis of the flow in hydraulic pipelines transporting spherical capsules for onshore applications. The analysis has been carried out with the aid of a well-validated computational fluid dynamics model for better understanding of the origins of the forces governing the entire unsteady capsule motion. The model has been validated against the experimental data obtained from the test rig been developed for this study. Multiple regression analysis has been used for the estimation of the effects of the various design parameters on the friction factor of capsules for onshore applications. Furthermore, pressure drop expressions have been formulated based on the prediction models. A novel prediction model has been developed to present the starting up energy requirements for capsule flow within the pipeline.

This study has employed a standard $k-\epsilon$ model in FLUENT to predict the flow characteristics when the flow is turbulent. The study has dealt with the effect of capsule rotation and position on the flow velocity and pressure and on the pressure drop variation across the test section. The study has also made the use of an advanced six degree of freedom simulation technique. This technique has been used for analyzing the transport of solid bodies in pipelines with much better accuracy. In this technique, the capsules have been treated as free bodies completely. The model developed in this study has the advantage of not requiring any inputs in terms of the capsule velocity or orientation. The hydrodynamic forces acting on the capsules has also been predicted. The computational expenses of such simulation techniques have been covered successfully by the massive computational power provided by the university's high performance workstation.

The specific innovative contributions of the numerical method developed here are: (1) the deforming unstructured mesh method is able to handle a rigid body undergoing relatively high displacement and (2) the

implemented spring-based re-meshing method used, which can significantly improve the computational efficiency.

REFERENCES

- [1]. Liu, H. Hydraulic behaviors of coal log flow in pipe. in 4th International Conference on Bulk Materials, Storage, Handling and Transportation: 7th International Symposium on Freight Pipelines; Preprints of Papers. 1992. Institution of Engineers, Australia.
- [2]. Subramanya, K., Pipeline transportation technology: An overview. *Current Science*, 1998. 75(8): p. 824-826.
- [3]. Asim, T., Computational Fluid Dynamics Based Diagnostics and Optimal Design of Hydraulic Capsule Pipelines. 2013, The University of Huddersfield.
- [4]. Deng, S., et al., A dynamic mesh strategy applied to the simulation of flapping wings. *International Journal for Numerical Methods in Engineering*, 2016.
- [5]. FLUENT, A., ANSYS Fluent UDF Manual, Release 15.0. 2013, ANSYS Inc.
- [6]. FLUENT, A., ANSYS FLUENT Theory Guide, Release 14.0, in ANSYS Inc., USA. 2011.
- [7]. Fluent, I., FLUENT 6.3 user's guide. *Fluent documentation*, 2006.
- [8]. Khalil, M.F., et al., Prediction of Lift and Drag Coefficients on Stationary Capsule in Pipeline. *CFD Letters*, 2009. 1(1): p. 15-28.
- [9]. Grinis, L. and U. Tzadka. Vortex Flow Past a Sphere in a Constant-Diameter Pipe. in *The Twenty-first International Offshore and Polar Engineering Conference*. 2011. International Society of Offshore and Polar Engineers.
- [10]. ANSYS, I., ANSYS Fluent Tutorial Guide. 2015.
- [11]. Munson, B., D. Young, and T. Okiishi, *Fundamentals of Fluid Mechanics*. 2002: New York: John Wiley & Sons Inc.
- [12]. Moody, L.F., Friction factors for pipe flow. *Trans. ASME*, 1944. 66(8): p. 671-684.